Data driven time alignment for TOF-PET

Ahmadreza Rezaei[1], Georg Schramm[1], Koenraad Van Laere[1], Johan Nuyts[1]

I. Introduction

The addition of time of flight (TOF) information in positron emission tomography (PET) reconstructions enables a more robust estimation of the tracer distribution uptake. Furthermore, it enables the estimation of the attenuation image from the PET data, if the spatial distribution of the activity is wider than the TOF resolution of the scanner. The use of TOF-PET data requires accurate alignment of the timing information, which is typically obtained by an additional acquisition of a known source of activity [1], from background LSO radiation [2] or from the clinical data [3]. In this work we propose a method to align the TOF data using the TOF-PET emission data, and we analyze the effects of an inaccurate TOF alignment on joint activity and attenuation reconstructions [4] in a uniform phantom scan as well as a patient $^{18}F-FDG$ brain scan.

II. Methods

Assuming a TOF shift δt_i along each line of response i we express the expected emission measurements as

$$y_{i,t+\delta t_i} = \sum_j c_{i,j}\bar{g}_{j,t+\delta t_i}\lambda_j + s_{i,t} \tag{1}$$

where $c_{i,j}$ is the sensitivity of LOR i to voxel j (accounting for the effects of attenuation and detector-pair sensitivities), $s_{i,t}$ is the average scatter and randoms contribution of the data-bin (i,t), λ is the activity distribution,

$$g_{j,t+\delta t_i} = e^{-(j-(t+\delta t_i))^2/2\sigma^2}/\sqrt{2\pi\sigma^2} \tag{2}$$

is the Gaussian TOF-kernel with a TOF-resolution of σ and TOF-index t, and where we used a somewhat inaccurate notation $j-t$ to denote the distance between the point corresponding to voxel j and the point corresponding to TOF-index t along LOR i, and $\bar{g}$ is the effective resolution of the scanner after convolving the Gaussian TOF-kernel g with the TOF bin-width.

The TOF shift along each individual LOR is computed by minimizing the quadratic differences between the emission measurements $y_{i,t}$ and the expected emission measurements $\bar{y}_{i,t+\delta t_i}$

$$Q = \sum_{i,t}\frac{1}{2}(y_{i,t}-\bar{y}_{i,t+\delta t_i})^2 \tag{3}$$

by setting the first derivative of (3) with respect to the TOF shifts δt_i to zero, i.e.

$$\frac{\partial Q}{\partial \delta t_i} = \sum_t (y_{i,t}-\bar{y}_{i,t+\delta t_i})\frac{\partial \bar{y}_{i,t+\delta t_i}}{\partial \delta t_i} = 0 \tag{4}$$

[1]Nuclear Medicine, KU Leuven, B-3000 Leuven, Belgium.

Approximating the TOF Gaussian distribution by its truncated Taylor's expansion

$$\bar{g}_{j,t+\delta t_i} \simeq \bar{g}_{j,t} + \delta t_i \bar{g}'_{j,t} \quad \text{with} \quad \bar{g}'_{j,t} = \frac{\partial \bar{g}_{j,t}}{\partial t} \tag{5}$$

the expected emission measurement and its derivative with respect to the TOF shifts δt_i can be written as

$$\begin{aligned} \bar{y}_{i,t+\delta t_i} &= \sum_j c_{i,j}\bar{g}_{i,t}\lambda_j + s_{i,t} + \delta t_i \sum_j c_{i,j}\bar{g}'_{i,t}\lambda_j \\ &= y_{i,t} + \delta t_i \bar{y}'_{i,t} \qquad (6) \\ \bar{y}'_{i,t} &= \frac{\partial \bar{y}_{i,t+\delta t_i}}{\partial \delta t_i} \qquad (7) \end{aligned}$$

Inserting (6) and (7) in (4) gives an expression for the residual TOF shifts along each LOR, which can be iterated to improve the estimate

$$\delta t_i = \frac{\sum_t (y_{i,t}-\bar{y}_{i,t})\bar{y}'_{i,t}}{\sum_t y'^2_{i,t}} \tag{8}$$

A. Crystal Shifts

To reduce the number of parameters, we assume that a time shift $\delta\tau_x$, relative to a global reference time, is associated to each crystal x, and that each individual LOR shift can be computed as the difference between the two corresponding crystal time shifts as proposed in [3]:

$$\delta t_{i(x,\psi)} = (-1)^{d_{x\to\psi}}(\delta\tau_x - \delta\tau_\psi) \tag{9}$$

where $i(x,\psi)$ is the LOR connecting crystals x and ψ and $d_{x\to\psi}$ determines the direction assigned to the LOR: $d_{x\to\psi}$ is zero if the LOR direction is from x to ψ and equal to 1 otherwise. The crystal time shifts are computed as

$$\hat{\delta\tau} = \underset{\delta\tau}{\operatorname{argmin}} \sum_{x,\psi,t}\frac{1}{2}(y_{i(x,\psi),t} - \bar{y}_{i(x,\psi),t+\delta t_{i(x,\psi)}})^2 \tag{10}$$

where $\hat{\delta\tau}$ is the set of estimated shifts $\hat{\delta\tau}_x$. The optimization involves the computation of fan sums for each crystal, i.e. summations over all LORs involving a particular crystal.

III. Experiment Design

Emission data from a uniform phantom scan as well as a brain ^{18}F-FDG patient scan were acquired using the GE SIGNA PET/MR scanner. The phantom and the patient were injected with 21 MBq and 152 MBq of the ^{18}F-FDG tracer and scanned for a duration of 10 and 20 minutes, respectively. The GE PET Reconstruction Toolbox (v1.28) was used to preprocess the raw emission data, and the expected scatter data were estimated using the vendor-provided atlas-based attenuation image. MLEM reconstructions were made. For the

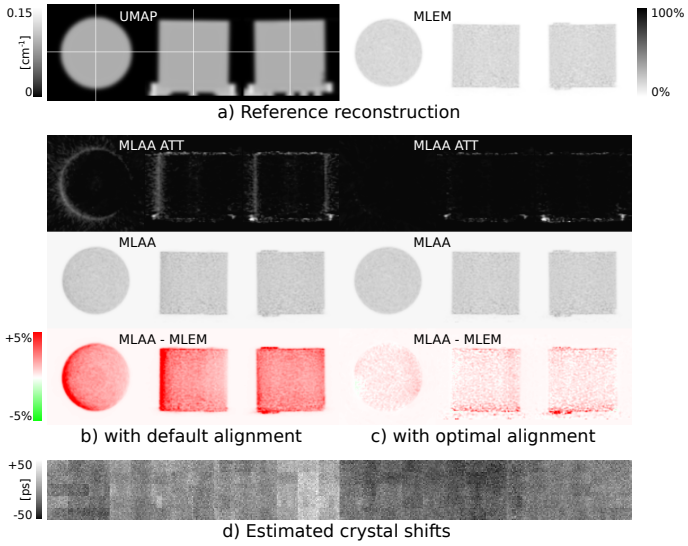

Fig. 1. Results of the phantom measurements. MLAA jointly estimated the activity and changes to the template based attenuation. UMAP: attenuation template. MLAA ATT: change to the attenuation computed by MLAA.

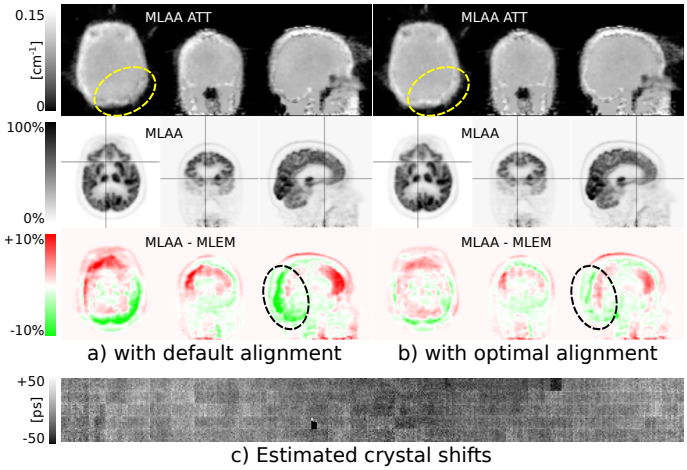

Fig. 2. Results of the Patient data. The MLEM reconstruction used the CT-based attenuation, MLAA jointly reconstructed the activity (MLAA) and attenuation (MLAA ATT).

phantom, an attenuation template was available which was used for attenuation correction. For the patient data, low dose (11 mAs) CT images were obtained using a Siemens HIREZ PET/CT scanner, aligned rigidly and used for attenuation correction. Also MLAA [4] reconstructions were computed, using 3 iterations and 32 subsets (updating the activity once and the attenuation twice in each iteration for MLAA). For the patient scan, the scale problem of MLAA was solved by incorporating an intensity prior favoring brain-tissue/zero attenuation within/outside the support of the activity during reconstructions as described in [5]. For the phantom, the vendor provided attenuation template was used during MLAA reconstruction and as a result, MLAA estimated the activity and additional small changes to this predefined attenuation map (instead of the full attenuation map). For ideal, consistent PET data, MLEM and MLAA should produce identical reconstructions. The differences of MLEM and MLAA activity distributions were analyzed as a surrogate for data consistency.

IV. Results

Figure 1 shows the reference MLEM activity reconstruction, MLAA reconstructions using the default (1b) and the proposed (1c) TOF alignments, the difference between the MLAA and MLEM reconstructions, and the crystal map of the estimated shifts (1d). Interestingly, the MLAA activity reconstruction using the uncorrected TOF alignment seems to be affected by an activity gradient (up to 5% of the activity). Furthermore, analyzing the residual MLAA attenuation reconstruction suggests a slight mis-alignment of the phantom to the emission data. The estimated crystal TOF-shifts are small but their distribution is structured (1d). The gradient and the residual MLAA attenuation reconstructions are no longer present after correcting for these residual crystal TOF shifts. In this study, the mean absolute value of the estimated TOF shifts was 9.6 ps.

Figure 2 shows MLAA activity and attenuation reconstructions with the default (2a) and the proposed (2b) alignment of the crystal TOF shifts, as well as the estimated crystal shifts (2b). Without correction of the additional TOF alignment, the differences between MLAA and MLEM activity images are similar to those observed for the phantom study. Close inspection of the MLAA attenuation reconstruction also reveals a gradient in the attenuation reconstruction which has negatively affected the reconstruction of the skull (highlighted in yellow). Overall, this results in strong changes in reconstructed posterior cortical and cerebellar FDG activity that are clinically highly relevant (up to 10%). With the additional TOF alignment correction the MLAA and MLEM reconstructions became more similar and the reconstruction of the skull improved. In this study, the mean absolute of the estimated TOF shifts was 10.0 ps.

V. Discussion and Conclusion

As previously observed, we find that MLAA reconstructions are more sensitive to data/modeling inconsistencies compared to MLEM reconstructions. This is because MLEM and MLAA have different degrees of freedom (while MLEM reconstructs only the activity, MLAA reconstructs an activity and attenuation pair) to explain the emission measurements. This can complicate the validation of MLAA using MLEM reconstructions for reference, but it also provides an opportunity to identify modeling or data correction inaccuracies. In this work, we propose a method inspired by [3] to better align the TOF emission measurements by correcting for a TOF shift along the measured LORs during reconstruction. For practical reasons, we used a crystal model and assigned TOF shifts to each of the scanner crystals which are used to determine the TOF shifts along the measured LOR. We demonstrated how these shifts can differently affect activity and attenuation reconstructions and are important for quantitative assessment of patient data.

VI. ACKNOWLEDGMENTS

This work was supported by the Research Foundation Flanders (FWO) 12T7118N and project G.0275.14N.

REFERENCES

[1] A. E. Perkins, M. Werner, A. Kuhn, S. Surti, G. Muehllehner, and J. S. Karp. "Time of Flight Coincidence Timing Calibration Techniques Using Radioactive Sources". *IEEE Nuclear Science Symposium Conference Record, 2005*. Vol. 5. Oct. 2005, pp. 2488–2491.

[2] H. Rothfuss, A. Moor, J. Young, V. Panin, and C. Hayden. "Time Alignment of Time of Flight Positron Emission Tomography Using the Background Activity of LSO". *2013 IEEE Nuclear Science Symposium and Medical Imaging Conference (2013 NSS/MIC)*. Oct. 2013, pp. 1–3.

[3] M. E. Werner and J. S. Karp. "TOF PET Offset Calibration from Clinical Data". en. *Phys. Med. Biol.* 58.12 (2013), p. 4031.

[4] Ahmadreza Rezaei, Michel Defrise, Girish Bal, Christian Michel, Maurizio Conti, Charles Watson, and Johan Nuyts. "Simultaneous Reconstruction of Activity and Attenuation in Time-of-Flight PET." *IEEE Trans. Med. Imaging* 31.12 (Dec. 2012), pp. 2224–33.

[5] Ahmadreza Rezaei, Georg Schramm, Gaspar Delso, Johan Nuyts, and Koenraad Van Laere. "A Quantitative Evaluation of Joint Activity and Attenuation Reconstruction in TOF-PET/MR Brain Studies". *PSMR 2017*.